The Effect of Silyl and Phenyl Functional Group End Caps on the Nonlinear Optical Properties of Polyynes: A Long-Range Corrected Density Functional Theory Study

ARTICLE *in* INTERNATIONAL JOURNAL OF QUANTUM CHEMISTRY · AUGUST 2009

Impact Factor: 1.43 · DOI: 10.1002/qua.22026

The Effect of Silyl and Phenyl Functional Group End Caps on the Nonlinear Optical Properties of Polyynes: A Long-Range Corrected Density Functional Theory Study

JONG-WON SONG,[1,2] MARK A. WATSON,[1,2] HIDEO SEKINO,[2,3] KIMIHIKO HIRAO[1,2]

[1] *Department of Applied Chemistry, School of Engineering, The University of Tokyo, Tokyo 113-8656, Japan*

[2] *CREST, Japan Science and Technology Agency, Saitama 332-0012, Japan*

[3] *Department of Knowledge-Based Information Engineering, Toyohashi University of Technology, Toyohashi 441-8580, Japan*

Received 9 November 2008; accepted 2 December 2008
Published online 6 March 2009 in Wiley InterScience (www.interscience.wiley.com).
DOI 10.1002/qua.22026

ABSTRACT: The polarizabilities, α, second-hyperpolarizabilities, γ, and γ scaling factors, c, of polyynes [i-$(Pr)_3$ Si–$(C{\equiv}C)_n$–Si i-$(Pr)_3$, H–$(C{\equiv}C)_n$–Si i-$(Pr)_3$, H–$(C{\equiv}C)_n$-Ph, and Ph–$(C{\equiv}C)_n$–Ph: n = 1 to 8] end-capped with triisopropylsilane (i-$(Pr)_3$ Si–; TIPS) and phenyl groups were calculated using HF and DFT using the recently developed LC-BOP and LCgau-BOP functionals. Comparison with the α and γ values of the uncapped polyynes shows that the TIPS and phenyl end caps do not increase the α and γ values by a simple additive constant, but instead seem to expand the effective conjugation length (n) of the polyyne backbone. Using a newly-proposed power-law function, $\gamma = a + b(n + \Delta n)^c$, we found that a single phenyl or TIPS end cap has the effect of increasing n by approximately Δn = 1.35 or 0.83, respectively. In the case of the phenyl end caps, we confirm that this function gives a better fit to the data than the function $\gamma = a + bn^c$, even with constant b and c values, determined from a fit to the uncapped polyyne γ values ($\gamma = bn^c$). In the case of the TIPS end caps, the fit to $\gamma = a$

Correspondence to: J-W. Song; e-mail: sjoshua@qcl.t.u-tokyo.ac.jp

Contract grant sponsor: Japan Science and Technology Agency (JST) (Core Research for Evolutional Science and Technology Program).

$+ b(n + \Delta n)^c$ gives a smaller Δn, but the assumption of constant b and c is less accurate. We also compared our c values to experimental data using the commonly used function $\gamma = a + bn^c$. Our results are consistent with the experimental c values, in that the c values of Ph–(C≡C)n–Ph are higher than those of i-(Pr)$_3$ Si–(C≡C)$_n$–Si i-(Pr)$_3$. Finally, using the power-law, $\gamma = a + b(n + \Delta n)^c$, we predict the, as yet undetermined, experimental c value of uncapped polyynes using the experimental γ values of Ph–(C≡C)$_n$–Ph ($\Delta n = 2.7$), to be ~4.88. Int J Quantum Chem 109: 2012–2022, 2009

Key words: nonlinear optical property; polyyne; long-range corrected; DFT; end cap

1. Introduction

Recently, there has been considerable interest in the development of organic conjugated materials with large nonlinear optical (NLO) properties because of their potential use in various optical devices [1–6]. For example, theoretical chemical calculations can be used to analyze the trend of molecular hyperpolarizabilities in well-defined organic molecules and polymers.

Density functional theory (DFT)[7–9] is one of the most widely-used quantum chemical methods because of its ability to calculate electron correlation effects with reasonable computational cost. However, it is well known that DFT significantly overestimates polarizabilities (α) and second-hyperpolarizabilities (γ) and gives catastrophically divergent values for long-chain conjugated molecules [10–12]. On the other hand, standard electron correlation methods such as MP2, CCSD, and CCSD(T) cannot currently be applied to very large molecules because of the high scaling of computational cost with system size.

Recently, we reported that DFT including the long-range correction scheme (LC)[13–16] does not suffer from the overestimation and catastrophic divergence of α and γ for long-chain polyynes and polyenes. Moreover, LC-DFT can solve many of the problems that conventional DFT confronts, such as the underestimation of Rydberg excitation energies and corresponding oscillator strengths [15], the poor reproduction of charge-transfer excitations in time-dependent DFT calculations [15], the underestimation of barrier heights [15], and the poor description of vander Waals interactions [17]. More recently, our improved LC scheme with a range separation including a short-range Gaussian attenuation, named LCgau, showed better performance in predicting thermochemical properties, such as atomization energies, reaction enthalpies and barrier heights, as well as excitation energies, including core excitation energies [18, 19].

There has been extensive interest in the NLO properties of long-chain molecules, in that they are expected to show not only high γ values but also a high γ scaling factor with respect to chain number (n). Recently, Eisler et al. [20, 21] reported experimental results that show that polyyne molecules [i-(Pr)$_3$ Si-(C≡C)$_n$-Si i-(Pr)$_3$] end-capped with triisopropylsilane (i-(Pr)$_3$ Si-; TIPS) have a surprisingly high γ scaling factor of 4.28. In their article, they assumed that the TIPS functional groups located at ends of the chain would have a simple additive effect on the γ values, and would not affect the size of the γ scaling factor. However, in our DFT investigations of the end-capped chains i-(Pr)$_3$ Si–(C≡C)$_n$–Si i-(Pr)$_3$ (n = 4, 5, 6, and 8) using X-ray crystal structures, we found that the addition of the TIPS functional groups can significantly change the size of the γ scaling factor. To rationalize this effect, we proposed that the end caps play a role in increasing the electron delocalization, thus increasing the effective conjugation length of the molecule [19].

However, to the best of our knowledge, this effect of the end caps on the hyperpolarizabilities of conjugated organic molecules seems to have been studied neither theoretically nor experimentally. We therefore decided to investigate this issue in more detail in this article. We proceed by calculating α, γ, and the γ scaling factors of long-chain polyynes end-capped with TIPS using LC-DFT, LCgau-DFT, as well as simple Hartree–Fock (HF) calculations. In addition, we also consider the phenyl group end caps comparing with recent experimental the γ scaling factors of long-chain polyynes end-capped with phenyl groups [22].

2. Theory

In the LC scheme [14], the electron repulsion operator, $1/r_{12}$, is divided into short- and long-range parts using a standard error function

$$\frac{1}{r_{12}} = \frac{1 - \mathrm{erf}(\mu r_{12})}{r_{12}} + \frac{\mathrm{erf}(\mu r_{12})}{r_{12}}, \quad (1)$$

where $r_{12} = \mathbf{r}_1 - \mathbf{r}_2$ is the distance between electrons $\mathbf{r}_1$ and $\mathbf{r}_2$, and m is a parameter that determines the proportion between the two ranges depending on the value of r_{12}. The first term of Eq. (1) is the short-range interaction term, and the second term is the long-range interaction term. The DFT exchange functional is included through the first term, and the long range orbital-orbital exchange interaction is described using the HF exchange integral.

In the LC scheme, the short-range exchange functional may be computed by modifying the usual exchange energy expression from,

$$E_x = -(1/2)\Sigma_\sigma \int \rho_\sigma^{4/3} K_\sigma d^3\mathbf{R}, \quad (2)$$

into

$$E_x^{sr,\mathrm{erf}} = -\frac{1}{2}\sum_\sigma \int \rho_\sigma^{4/3} K_\sigma \times \left\{1 - \frac{8}{3} a_\sigma \left[\sqrt{\pi}\,\mathrm{erf}\left(\frac{1}{2a_\sigma}\right) + 2a_\sigma(b_\sigma - c_\sigma)\right]\right\} d^3\mathbf{R}, \quad (3)$$

where a_σ, b_σ, and c_σ are defined as

$$a_\sigma = \frac{\mu}{6\sqrt{\pi}} \rho_\sigma^{-1/3} K_\sigma^{1/2}, \quad (4)$$

$$b_\sigma = \exp\left(-\frac{1}{4a_\sigma^2}\right) - 1, \quad (5)$$

and

$$c_\sigma = 2a_\sigma^2 b_\sigma + \frac{1}{2}. \quad (6)$$

K_σ is called the enhancement factor, and the use of K_σ allows the modification of generalized gradient approximation functionals.

Recently we developed a new scheme using the separation [18],

$$\frac{1}{r_{12}} = \frac{\mathrm{erfc}(\mu r_{12})}{r_{12}} - k\frac{2\mu}{\sqrt{\pi}} e^{-(1/a)\mu^2 r_{12}^2} + \frac{\mathrm{erf}(\mu r_{12})}{r_{12}} + k\frac{2\mu}{\sqrt{\pi}} e^{-(1/a)\mu^2 r_{12}^2}. \quad (7)$$

Like the LC scheme, the first two terms of Eq. (7) are the short-range interaction terms, and the third and fourth terms are the long-range interaction terms. Note that the sign of the parameter k is reversed when compared with our previous article [18]. We referred to this new long-range corrected method as LCgau-DFT. The Gaussian correction gives an additional contribution to the short-range exchange energy of a very similar form to Eq. (3)

$$E_x^{sr.\mathrm{gau}} = -\frac{1}{2}k\sum_\sigma \int \rho_\sigma^{4/3} K_\sigma \times \frac{8}{3} a_\sigma \left[\sqrt{\pi}\,\mathrm{erf}\left(\frac{1}{2d_\sigma}\right) + (2d_\sigma - 16d_\sigma^3)e_\sigma - 4d_\sigma\right] d^3\mathbf{R}, \quad (8)$$

where d_σ and e_σ are defined as

$$d_\sigma = \frac{a_\sigma}{\sqrt{a}}, \quad (9)$$

$$e_\sigma = \exp\left(-\frac{1}{4d_\sigma^2}\right) - 1, \quad (10)$$

and the total short-range DFT exchange energy of the LCgau scheme may be obtained as a summation of two contributions,

$$E_x^{sr} = E_x^{sr,\mathrm{erf}} + E_x^{sr,\mathrm{gau}}.$$

In the case of the LC scheme, exact HF exchange is incorporated in the long-range region via integrals such as

$$E_x^{\mathrm{lr,LC}} = -\frac{1}{2}\sum_\sigma \sum_i^{\mathrm{occ}} \sum_j^{\mathrm{occ}} \int\int \psi_{i\sigma}^*(\mathbf{r}_1)\psi_{j\sigma}(\mathbf{r}_1) \times \left[\frac{\mathrm{erf}(\mu r_{12})}{r_{12}}\right] \psi_{i\sigma}(\mathbf{r}_2)\psi_{j\sigma}^*(\mathbf{r}_2) d^3\mathbf{r}_1 d^3\mathbf{r}_2, \quad (11)$$

and, in the case of the LCgau scheme,

$$E_x^{\mathrm{lr,LCgau}} = -\frac{1}{2}\sum_{\sigma}\sum_{i}^{\mathrm{occ}}\sum_{j}^{\mathrm{occ}}\int\int \psi_{i\sigma}^{*}(\mathbf{r}_1)\psi_{j\sigma}(\mathbf{r}_1) \times \left[\frac{\mathrm{erf}(\mu r_{12})}{r_{12}} + k\frac{2\mu}{\sqrt{\pi}}e^{-(1/a)\mu^2 r_{12}^2}\right]\psi_{i\sigma}(\mathbf{r}_2)\psi_{j\sigma}^{*}(\mathbf{r}_2)d^3\mathbf{r}_1 d^3\mathbf{r}_2, \quad (12)$$

where $\psi_{i\sigma}$ is the ith σ-spin molecular orbital.

3. Computational Details

We first computed the α and γ values of the single-capped polyynes, H–(C≡C)$_n$–Si i-(Pr)$_3$, and double-capped polyynes, i-(Pr)$_3$ Si–(C≡C)$_n$–Si i-(Pr)$_3$ (n = 1–8) using HF and LC-DFT. The calculations were repeated using the phenyl end caps for H–(C≡C)$_n$–Ph and Ph–(C≡C)$_n$–Ph (n = 1–8). In the LC scheme, the range-separation parameter was chosen as μ = 0.47 [16], and in the LCgau scheme, we used the optimized parameters [18], μ = 0.42, α = 0.011, and k = 18.0. The LC methods were used in conjunction with the B88 exchange functional [23] and the one-parameter progressive correlation functional [24] (LC-BOP and LCgau-BOP).

In our previous theoretical study of H–(C≡C)$_n$–H, we reported that the α and γ values obtained using LC-BOP and LCgau-BOP (with the above parameters) were in good agreement with those obtained by the CCSD(T) method [13]. For comparison, we also calculated the α and γ values using HF, which has been used previously by many researchers. Although HF does not include electron correlation effects, it has been shown to give very similar results to CCSD(T) benchmarks for the calculation of α values of polyynes [13]. However, we note that HF has been shown to somewhat underestimate γ values in long-chain polyynes, while LC-BOP is generally closer to the benchmark CCSD(T) results [13].

The geometries of the polyyne backbones are the same as those used in Ref. [13]. That is, the single (C—C) and triple (C≡C) bond lengths (C—C: 1.3650 Å; C≡C: 1.2050 Å) are average experimental values obtained from the i-(Pr)$_3$ Si–(C≡C)$_n$–Si i-(Pr)$_3$ X-ray diffraction data for n = 4, 5, 6, and 8 [21].

For the TIPS end cap, we used the crystal structure taken from the i-(Pr)$_3$ Si–(C≡C)$_n$–Si i-(Pr)$_3$ molecule of Ref. [21]. This was attached to the end of the polyyne chains at either or both ends, without further geometry optimization, because it is reasonable to expect that the precise geometry of the TIPS end cap will not substantially affect the α or γ values.

For the phenyl end cap, we used the geometry of the phenylacetylene (C_6H_5—C≡CH) molecule in the NIST-JANAF tables [25]. In detail, we attached the geometry optimized at the CCSD/6-31G** level of theory, which is the optimized geometry using the highest level of calculation in the NIST-JANAF tables, to the long-chain polyynes without further optimization. The phenyl-polyyne C—C bond length is 1.4415Å, which is not so different from the experimental bond length, 1.435Å, reported in Ref. 21. When attaching two phenyl groups, they are positioned to lie in the same plane.

The α and γ values were computed by the finite-field (FF) method with numerical Romberg iteration [26] using field strengths of $\pm 0.0016 \times 2^k$AU (atomic unit) along the Z axis (the line joining the carbon atoms in the polyyne backbone), for k in the range 0 to 4. We also used a high self consistent field (SCF) convergence threshold of 10^{-12}–10^{-9} as the numerical differentiation requires high accuracy in the total energy, where the lowest threshold was used for the shortest chains: for n = 1–3, 10^{-12}, for n = 4–6, 10^{-11}, for n = 7, 10^{-10} and for n = 8, 10^{-9} was used. In all calculations, the cc-pVDZ basis set [27] was used. All calculations were performed using a development version of the Gaussian 03 program [28] where we have implemented the LC and LCgau schemes. All results are given in atomic units unless otherwise stated.

4. Results and Discussion

4.1. The Effect of the TIPS (i-Pr$_3$ Si—) and Phenyl (C_6H_5—) End Caps on the α and γ Values of Polyynes

Figures 1(a) and (b) and Tables I and II show the α and γ values of H–(C≡C)$_n$–Si i-(Pr)$_3$ and i-(Pr)$_3$ Si–(C≡C)$_n$–Si i-(Pr)$_3$, calculated using HF, LC-BOP, and LCgau-BOP. Generally, it can be seen that HF gives the lowest α and γ values, whereas LC-BOP gives slightly larger values, and LCgau-BOP gives the largest values. As n is increased, the differences among the methods for both the α and γ values become larger, but agreement is generally good between the methods.

Concerning the effect of the end caps, it is clear that the TIPS group has an elevating effect on the α and γ values in polyynes. In fact, the TIPS end cap

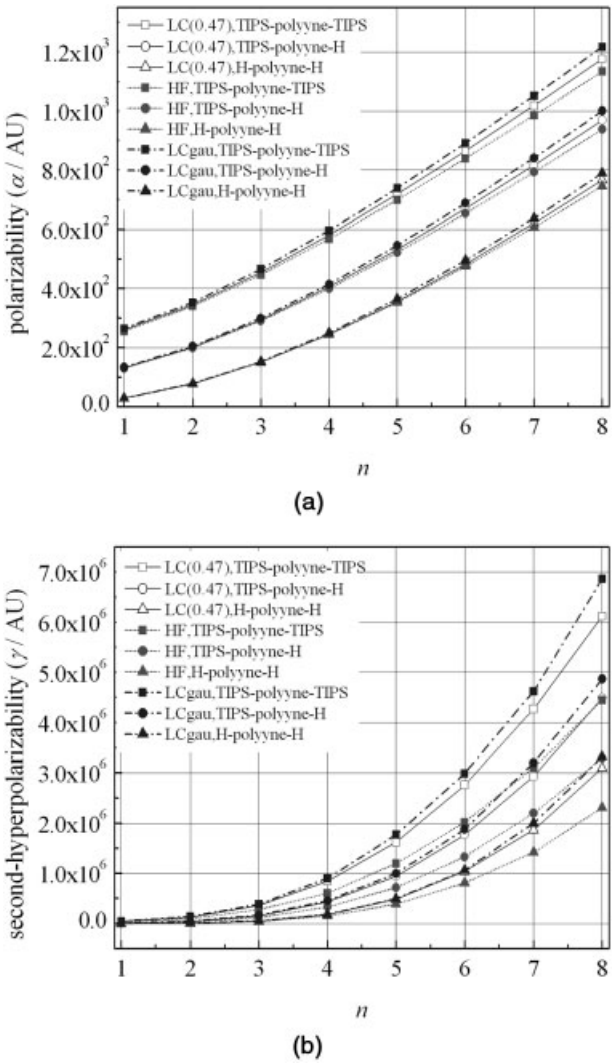

FIGURE 1. (a) The polarizabilities, α, and (b) second-hyperpolarizabilities, γ of the polyynes [H–(C≡C)$_n$–H, H–(C≡C)$_n$–Si *i*-(Pr)$_3$, and *i*-(Pr)$_3$ Si–(C≡C)$_n$–Si *i*-(Pr)$_3$] calculated using LC-BOP, HF, and LCgau-BOP.

seems to increase the effective length of the polyyne chain. As the dependence of the α values on n is approximately linear, this corresponds to an increase in the α values by an approximately constant amount. However, this is markedly not the case with the γ values, which increase in a strongly nonlinear fashion with n. That is, the effect of the end caps is not a simple additive constant to the γ values. Specifically, a single TIPS group shifts the α values according to a change in n of $\Delta n = 1.2$–1.5 in all the methods we used. In the case of the γ values, the effect of one TIPS group seems to increase the effective chain length by $\Delta n = 0.8$ in all the methods we used.

For comparison, we calculated the α and γ values of the phenyl end-capped polyynes [H–(C≡C)$_n$–Ph and Ph–(C≡C)$_n$–Ph] using HF, LC-BOP, and LCgau-BOP (Tables I and II). Figures 2(a) and (b) show, respectively, the α and γ values of H–(C≡C)$_n$–Si *i*-(Pr)$_3$, *i*-(Pr)$_3$ Si–(C≡C)$_n$–Si *i*-(Pr)$_3$, H–(C≡C)$_n$–Ph, and Ph–(C≡C)$_n$–Ph calculated using LCgau-BOP. We present only LCgau-BOP values to make it easy to differentiate the effects of the phenyl and TIPS end caps. As with the TIPS result, the phenyl group seems to increase the effective conjugation length of the polyyne backbone, but the effect seems to be somewhat stronger than with the TIPS end caps. Specifically, In the case of the γ values, the effect of one phenyl group is to increase the effective chain length by $\Delta n = 1.6$ in all cases.

To confirm the quality of our HF and DFT calculations, we decided to benchmark our results against data from rigorous wavefunction-based electron correlation methods, but because of the high computational expense, we only considered the smallest Ph-C≡C-Ph molecule. The resulting γ values were found to be 3.56×10^5, 3.04×105, 3.15×105, 3.06×105, and 3.47×105, using MP2, MP3, MP4SDQ, CCSD, and CCSD(T), respectively. These values are in good agreement with the LCgau-BOP, LC-BOP, and HF γ values (3.10×10^5, 3.06×10^5, and 2.37×10^5, respectively), although we may note that the HF result (which lacks electron correlation) is somewhat lower than the other values.

4.2. ESTIMATION OF THE Δn VALUE USING A POWER-LAW FUNCTION

Eisler et al. [20, 21] estimated the c values of *i*-(Pr)$_3$ Si–(C≡C)$_n$–Si *i*-(Pr)$_3$ using the power-law function, $\gamma = a + bn^c$, with the assumption that the TIPS end caps would give no additional electron delocalization effect, but rather a constant additive effect on the γ values. However, from our previous discussion, it is clear that the end caps do not have a constant additive effect. Indeed, it seems that a more physically motivated model should include a consideration of the change in effective conjugation length through Δn.

We therefore propose an alternative model for a comparison of the α, γ, and c values of the polyynes with different end caps, of the form $\gamma = a + b(n + \Delta n)^c$. The α value is intended to model the simple additive effect of the end caps, whereas Δn incor-

TABLE I

The longitudinal polarizabilities (α/AU) of the polyynes [H—(C≡C)$_n$–Si *i*-(Pr)$_3$, *i*-(Pr)$_3$Si–(C≡C)$_n$–Si *i*-(Pr)$_3$, H–(C≡C)$_n$–Ph, and Ph–(C≡C)$_n$–Ph] according to the chain numbers.

Molecule		1	2	3	4	5	6	7	8
H—(C≡C)$_n$–H	HF	29.44	78.91	151.78	244.56	353.59	475.35	606.90	745.81
	LC-BOP	28.93	77.86	150.98	245.25	357.18	483.24	620.37	765.96
	LCgau-BOP	29.15	78.72	153.24	249.86	365.14	495.56	637.92	789.58
H–(C≡C)$_n$–Si *i*-(Pr)$_3$	HF	130.97	199.96	291.35	399.96	521.79	653.64	792.99	937.97
	LC-BOP	132.02	201.42	294.46	406.06	532.30	669.83	815.98	968.64
	LCgau-BOP	133.97	204.85	300.35	415.41	546.09	688.96	841.21	1000.72
i-(Pr)$_3$Si–(C≡C)$_n$–Si *i*-(Pr)$_3$	HF	255.92	340.55	447.06	568.19	699.92	839.53	984.90	1134.51
	LC-BOP	260.10	346.00	455.51	581.03	718.50	864.95	1018.10	1176.29
	LCgau-BOP	264.96	353.22	466.28	596.27	739.11	891.76	1051.81	1217.34
H–(C≡C)$_n$–Ph	HF	125.56	204.11	302.29	415.81	541.25	675.73	817.07	963.41
	LC-BOP	125.25	204.11	303.81	420.29	550.12	690.30	838.39	992.49
	LCgau-BOP	126.72	207.20	309.50	429.59	564.00	709.66	864.01	1024.97
Ph–(C≡C)$_n$–Ph	HF	264.53	364.54	480.09	607.61	744.18	862.93	1035.48	1187.15
	LC-BOP	265.38	366.94	485.47	617.44	759.77	909.91	1065.83	1225.98
	LCgau-BOP	269.63	374.00	496.32	633.01	780.95	937.50	1100.47	1268.22

porates the effects of additional electron delocalization in the polyyne backbone. Because of the extra parameter Δn in this model, it is natural to expect a closer fit to the data, if full freedom is allowed in the parameter fitting. However, to minimize the fitting task and to simplify the model, we decided to hold the b and c values constant. That is, the data for the H–(C≡C)$_n$–H chain (n = 1 to 8) was first fitted to

TABLE II

The longitudinal second hyperpolarizabilities (γ/AU) of the polyynes [H–(C≡C)$_n$–Si *i*-(Pr)$_3$, *i*-(Pr)$_3$Si–(C≡C)$_n$–Si *i*-(Pr)$_3$, H–(C≡C)$_n$–Ph, and Ph–(C≡C)$_n$–Ph] according to the chain numbers.

Molecule		1	2	3	4	5	6	7	8
H–(C≡C)$_n$–H	LC-BOP	2.43×10^2	9.20×10^3	4.98×10^4	1.81×10^5	4.85×10^5	1.04×10^6	1.87×10^6	3.10×10^6
	LCgau-BOP	3.68×10^2	8.85×10^3	5.25×10^4	1.83×10^5	4.97×10^5	1.06×10^6	2.00×10^6	3.32×10^6
	HF	2.42×10^2	6.63×10^3	4.20×10^4	1.50×10^5	3.87×10^5	8.08×10^5	1.42×10^6	2.31×10^6
H–(C≡C)$_n$–Si *i*-(Pr)$_3$	LC-BOP	8.42×10^3	4.16×10^4	1.56×10^5	4.35×10^5	9.43×10^5	1.77×10^6	2.93×10^6	4.49×10^6
	LCgau-BOP	9.31×10^3	4.44×10^4	1.66×10^5	4.55×10^5	1.00×10^6	1.88×10^6	3.20×10^6	4.87×10^6
	HF	7.40×10^3	3.33×10^4	1.22×10^5	3.31×10^5	7.20×10^5	1.33×10^6	2.20×10^6	3.29×10^6
i-(Pr)$_3$Si–(C≡C)$_n$–Si *i*-(Pr)$_3$	LC-BOP	4.79×10^4	1.25×10^5	3.68×10^5	8.45×10^5	1.62×10^6	2.76×10^6	4.27×10^6	6.12×10^6
	LCgau-BOP	4.71×10^4	1.40×10^5	3.83×10^5	9.04×10^5	1.77×10^6	2.99×10^6	4.62×10^6	6.87×10^6
	HF	3.05×10^4	9.72×10^4	2.80×10^5	6.05×10^5	1.20×10^6	2.02×10^6	3.10×10^6	4.45×10^6
H–(C≡C)$_n$–Ph	LC-BOP	2.57×10^4	1.11×10^5	3.40×10^5	7.58×10^5	1.44×10^6	2.45×10^6	3.82×10^6	5.57×10^6
	LCgau-BOP	2.25×10^4	1.25×10^5	3.54×10^5	7.94×10^5	1.53×10^6	2.62×10^6	4.11×10^6	6.11×10^6
	HF	2.32×10^4	8.79×10^4	2.80×10^5	6.14×10^5	1.14×10^6	1.90×10^6	2.83×10^6	4.15×10^6
Ph–(C≡C)$_n$–Ph	LC-BOP	3.06×10^5	6.22×10^5	1.18×10^6	1.95×10^6	3.08×10^6	4.58×10^6	6.70×10^6	9.95×10^6
	LCgau-BOP	3.10×10^5	6.72×10^5	1.25×10^6	2.10×10^6	3.34×10^6	4.97×10^6	7.30×10^6	1.08×10^7
	HF	2.37×10^5	5.01×10^5	9.42×10^5	1.55×10^6	2.39×10^6	3.46×10^6	5.36×10^6	7.48×10^6

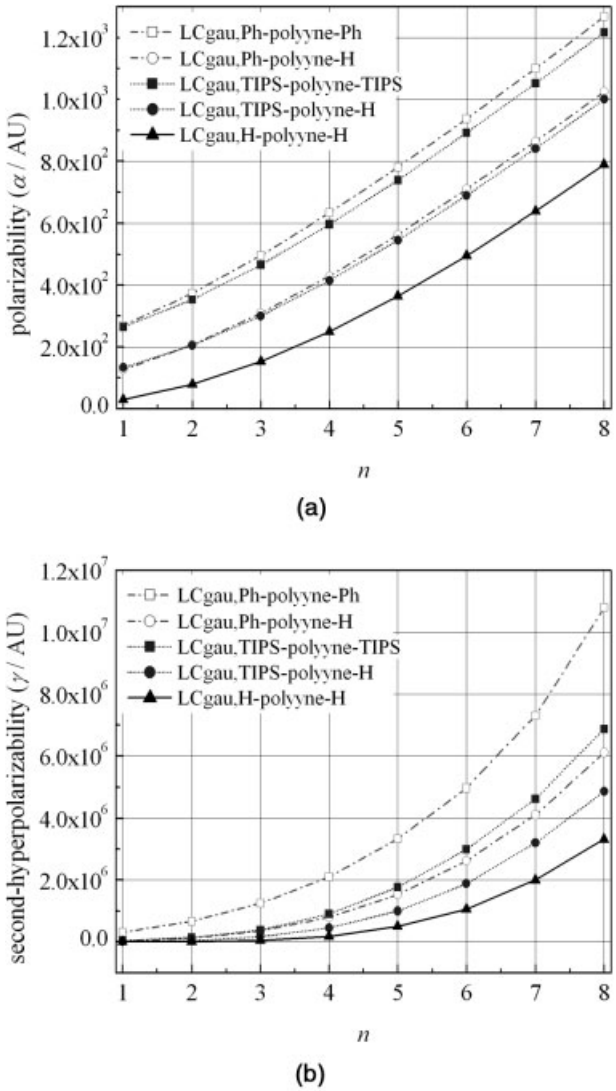

FIGURE 2. (a) The polarizabilities, α, and (b) second-hyperpolarizabilities, γ, of the polyynes [H–(C≡C)$_n$–H, H–(C≡C)$_n$–Si *i*-(Pr)$_3$, and *i*-(Pr)$_3$Si–(C≡C)$_n$–Si *i*-(Pr)$_3$, H–(C≡C)$_n$–Ph, and Ph–(C≡C)$_n$–Ph] calculated using LCgau-BOP.

the function $\gamma = bn^c$, where α and Δn are zero by definition. We then use these b and c values to obtain a fit to the power-law function of $\gamma = a + b(n + \Delta n)^c$ to obtain Δn for the end-capped molecules (Table III). All fitting was performed using the Levenberg–Marquardt algorithm and the Origin7.5 software package.

As a result, we obtained Δn values for the singly-capped molecules H–(C≡C)$_n$–Si *i*-(Pr)$_3$ of 0.83, 0.84, and 0.83, using data from the HF, LC-BOP, and LCgau-BOP calculations, respectively. The corresponding Δn values for the doubly-capped molecules *i*-(Pr)$_3$ Si–(C≡C)$_n$–Si *i*-(Pr)$_3$ were 1.58, 1.62, and 1.57, respectively. We see that the HF Δn value is the lowest of the three methods, but nevertheless, the Δn values seem to be approximately independent of the particular theoretical method. In summary, we see that one TIPS end cap seems to act like an additional –(C≡C)$_{0.83}$– group with respect to the g properties of polyynes.

Next, we obtained Δn for the phenyl end caps. For the singly-capped molecules, the corresponding Δn values were 1.33, 1.34, and 1.37, for HF, LC-BOP, and LCgau-BOP, respectively. For the doubly-capped molecules, the Δn values were 2.70, 2.66, and 2.89, respectively. Again, the Δn values are approximately independent of the particular theoretical method. In summary, we see that one phenyl end cap seems to act like an additional –(C≡C)$_{1.35}$– group with respect to the γ properties of polyynes.

We can measure the quality of the data fitting by inspection of the chi-square (χ^2) value, given for each data set in Tables III and IV. In the case of the Ph–(C≡C)$_n$–Ph chains, we can see that the $\gamma = a + b(n + \Delta n)^c$ model is somewhat better (with constant b and c) and has a χ^2 value smaller than the $\gamma = a + bn^c$ model (optimizing all three parameters). This supports the hypothesis that the phenyl end cap increases the effective conjugation length of the polyyne backbone, without significantly changing the basic c value.

However, in the case of the *i*-(Pr)$_3$ Si–(C≡C)$_n$–Si *i*-(Pr)$_3$ chains, the χ^2 value when fitting with the function $\gamma = a + b(n + \Delta n)^c$, keeping b and c constant, is greater than when fitting with $\gamma = a + bn^c$. This shows that the b and c values cannot be exactly transferred from the uncapped polyyne chain in this case, although this assumption is approximately true. Thus, although the new model appears to be a useful rationalization for the phenyl end caps, for a more accurate fitting of the data in the case of the TIPS end caps, the b and c values should be allowed to vary freely. However, though the $\gamma = a + bn^c$ model gives a better fit to the data, we emphasize that the result is not simply an additive constant to the basic $\gamma = bn^c$ model for polyynes because b and c must also change.

4.3. COMPARISON BETWEEN THE THEORETICAL AND EXPERIMENTAL RESULTS FOR POLYYNES

In this section, we consider the comparison of our theoretical results with experimental data ob-

TABLE III

The b, c, and χ^2 values of the γ power-law, $\gamma = bn^c$, of H–(C≡C)$_n$–H and the Δn and χ^2 values of the γ power-law, $\gamma = a + b(n + \Delta n)^c$, of H–(C≡C)$_n$–Si i-(Pr)$_3$, i-(Pr)$_3$Si–(C≡C)$_n$–Si i-(Pr)$_3$, H–(C≡C)$_n$–Ph, and Ph–(C≡C)$_n$–Ph.

Molecule		LC-BOP	LCgau-BOP	HF
		Electronic γ		
H–(C≡C)$_n$–H	b	978.3	850.4	970.8
	c	3.88 (±0.049)	3.98 (±0.053)	3.74 (±0.050)
	χ^2(*10^8)	4.12	5.21	2.66
H–(C≡C)$_n$–Si i-(Pr)$_3$	Δn	0.83 (±0.029)	0.84 (±0.035)	0.83 (±0.033)
	χ^2(*10^8)	30.2	52.9	18.9
i-(Pr)$_3$Si–(C≡C)$_n$–Si i-(Pr)$_3$	Δn	1.58 (±0.057)	1.62 (±0.045)	1.57 (±0.029)
	χ^2(*10^8)	179	142	61.8
H–(C≡C)$_n$–Ph	Δn	1.33 (±0.054)	1.34 (±0.049)	1.37 (±0.057)
	χ^2(*10^8)	139	145	76.0
Ph–(C≡C)$_n$–Ph	Δn	2.70 (±0.036)	2.66 (±0.039)	2.89 (±0.036)
	χ^2(*10^8)	124	187	65.6

The values in parentheses are estimates of the fitting error in each method.

tained from studies on the long-chain molecules Ph–(C≡C)$_n$–Ph and i-(Pr)$_3$ Si–(C≡C)$_n$–Si i-(Pr)$_3$ [22]. It is well known that the comparison of absolute γ values between different experimental groups can be problematic due to the dependence of the results on the experimental method employed. As a result, the most commonly used figure of merit when comparing the NLO properties of different molecular systems is the scaling factor c [20, 21]. We therefore focus on the comparison of the theoretical and experimental c values here.

In the experimental work [21, 22], the γ values for i-(Pr)$_3$ Si–(C≡C)$_n$–Si i-(Pr)$_3$ and Ph–(C≡C)$_n$–Ph were fitted to a model of the form $\gamma = a + bn^c$ to determine the scaling factors c. For consistency, we therefore used this model, but refitted the experi-

TABLE IV

The c and χ^2 values fitted using the γ power-law, $\gamma = a + bn^c$, of the polyynes [i-(Pr)$_3$Si–(C≡C)$_n$–Si i-(Pr)$_3$ and Ph–(C≡C)$_n$–Ph].

Molecule		LC-BOP	LCgau-BOP	HF	LC-BOP	LCgau-BOP	HF	Exp
		Electronic γ			Electronic γ + vibrational γ[a]			
i-(Pr)$_3$Si-(C≡C)$_n$-Si i-(Pr)$_3$	c	2.80 (±0.042)	2.92 (±0.011)	2.79 (±0.041)	2.89 (±0.035)	2.87 (±0.053)	2.83 (±0.074)	4.51 (±0.053)
	χ^2(*10^8)	12.2	5.60	4.54	3.98	10.8	9.67	0.261
Ph-(C≡C)$_n$-Ph	c	2.77 (±0.130)	2.76 (±0.122)	2.66 (±0.114)	2.58 (±0.071)	2.60 (±0.067)	2.80 (±0.228)	3.57 (±0.143)
	χ^2(*10^8)	281	296	134	39.1	40.9	225	1.69

Results are given using the electronic γ with and without vibrational corrections. The values in parentheses are estimates of the fitting error in each method.

[a] We used the vibrational γ values of polyyne of n = 2-7.

mental and theoretical γ data using the same fitting algorithm (Levenberg-Marquardt) to ensure a consistent comparison. The results are given in Table IV. It can be seen that the theoretical values are considerably lower than the experimental values. In the case of *i*-$(Pr)_3$ Si–$(C{\equiv}C)_n$–Si *i*-$(Pr)_3$, the *c* value from the LCgau-BOP calculations, which is the highest of the three methods considered, is 2.92. In contrast, the experimental *c* value is 4.51. In the case of the phenyl end caps, the *c* value using LCgau-BOP is 2.76, whereas the experimental value (c = 3.57) is somewhat larger.

However, there are several factors we have not considered thus far, which should be taken into account when comparing theory and experiment. Firstly, the experimentally measured quantity is the isotropic γ value, γ_{iso}, which is the rotational average of the full γ tensor. Secondly, it is well known that vibrational contributions to the total γ value can be significant, and it is possible to estimate these effects. Thirdly, the experimental measurements are taken in solution. The inclusion of solvent effects in our calculations is therefore also necessary.

Concerning the rotational averaging of the γ values, we calculated γ_{iso} for Ph-C≡C–Ph, Ph–$(C{\equiv}C)_3$–Ph, and Ph–$(C{\equiv}C)_5$–Ph at the HF level using the Dalton2.0 program package [29], which can accurately and efficiently compute all components of the full γ tensor using analytical energy derivatives. For Ph–C≡C–Ph, Ph–$(C{\equiv}C)_3$–Ph, and Ph–$(C{\equiv}C)_5$–Ph, we obtained γ iso values of 4.86×10^4, 1.90×10^5, and 4.80×10^5, respectively. The corresponding ratios of the longitudinal γ values (γ_{zzzz}) to giso were therefore found to be approximately $\gamma_{zzzz}/\gamma_{iso} = 5$ (more precisely, 4.88, 4.96, and 4.98, respectively). An exact ratio of 5 can be expected from theoretical considerations in the limit where the longitudinal component is much larger than all the other components. If we assume that the ratio $\gamma_{zzzz}/\gamma_{iso}$ is also ~5 for all the LC and LCgau calculations of Ph–$(C{\equiv}C)_n$–Ph and *i*-$(Pr)_3$ Si–$(C{\equiv}C)_n$–Si *i*-$(Pr)_3$, we can conclude that the *c* values computed above will not be changed. However, the absolute γ values will be reduced, and, in summary, we can see that all the values obtained in this study are then somewhat closer to experiment, being ~2 to 8 times too large.

Nevertheless, this discrepancy is still rather significant, and we therefore also considered the contribution to the total γ value due to vibration in the polyyne backbone. The experimental data was obtained using a differential optical Kerr effect apparatus [21, 30]. To estimate the vibrational γ (γ_{vib}) for Ph–$(C{\equiv}C)_n$–Ph and *i*-$(Pr)_3$ Si–$(C{\equiv}C)_n$–Si *i*-$(Pr)_3$, we therefore used the dc-Kerr expression previously given by Kirtman and coworkers [31, 32] within the double harmonic approximation, combined with data presented in Table I of Ref. 31 for long-chain polyyne molecules at the RHF/6-31G level of theory. Our resulting estimates of the ratio ($\gamma_{vib}/\gamma_{zzzz}$) between gvib and the electronic γ were found to be 6.24, 0.48, 0.36, 0.33, 0.32, 0.32, and 0.32 for n = 1–7, respectively. We can see that the vibrational effects will therefore increase our theoretical values, but not substantially (except for n = 1). Moreover, it seems that they cannot explain why our theoretical g values are larger than the experimental values of *i*-$(Pr)_3$ Si–$(C{\equiv}C)_n$–Si *i*-$(Pr)_3$ and Ph–$(C{\equiv}C)_n$–Ph, although we note that the vibrational effects of the end caps have not been considered which perhaps can alter the conclusion. Concerning the effect of the vibrational corrections, modified *c* values were obtained by refitting the corrected γ values to $\gamma = a + bn^c$. The results are given in Table IV. We can see that their inclusion has no systematic effect on the *c* values, and indeed, the correction is rather small. The resulting *c* values remain much lower than experiment.

So far, as the HF and LC-DFT results are close to the CCSD(T) benchmarks (see Section 4.1), we conclude that the gas phase calculations of the electronic component of the molecular γ values we present here are rigorous. However, as it was reported that even the CCSD(T) γ values are not converged with respect to the inclusion of correlation effects [13], we cannot ignore the errors resulting from the theoretical methods themselves. In addition, we acknowledge that the cc-pVDZ basis set used in our calculations is somewhat too small to accurately describe the γ values in our study [33, 34] and may account for the some of the discrepancy with experiment. However, from the above discussion, we are inclined to conclude that the major reason for the remaining discrepancy is the neglect of solvent effects, which are known to be important for the accurate reproduction of experimental data [35].

Nevertheless, though our theoretical *c* values are clearly much smaller than experiment, we believe our results are an improvement on previous theoretical studies, which report *c* values for H–$(C{\equiv}C)_n$–H in the range 1.26–3.3 [33, 36, 37]. In fact, our LC-DFT *c* values for the uncapped polyynes are somewhat higher than all other theoretical reports we are aware of [13]. We note that we

used improved geometries that were derived from x-ray crystal structures and included longer chain lengths up to $n = 8$, which can strongly influence the precise c values obtained. Finally, we can emphasize that although the theoretical c values are too low compared to the experimental c values, the qualitative trend in the experimental data is recovered correctly. That is, the addition of the end caps lowers the c values, and the phenyl caps have a greater influence than the TIPS caps [21].

Finally, we end this section with a prediction of the c value of the uncapped polyynes, H–(C≡C)$_n$–H, which has yet to be determined experimentally, using our model from Section 4.2. We showed that the function $\gamma = a + b(n + \Delta n)^c$ gives an accurate fit of the theoretical data for the phenyl end caps, using a constant c value, with or without end caps. Specifically, we obtained $\Delta n = 2.7$. If we assume this value is transferable, we can therefore fit the experimental γ values of Ph–(C≡C)$_n$–Ph to the function $\gamma = a + b(n + 2.7)^c$. The result, after optimizing a, b, and c, predicts the experimental γ scaling factor of H–(C≡C)$_n$–H to be 4.88 ($\pm$0.306), which is much larger than with the end caps.

5. Conclusions

We have studied the polarizabilities, α, second-hyperpolarizabilities, γ, and γ scaling factors, c, of polyynes using HF and DFT using the recently developed LC-BOP, and LCgau-BOP functionals. In particular, we have studied the effect on these NLO properties of the addition of TIPS and phenyl end caps to the polyyne backbone. We have shown that the end caps increase the α and γ values, but that this is not a simple additive effect compared to the uncapped polyynes.

We have explored a new power-law for the behavior of the γ values with respect to increasing chain length in the presence of end caps. Our approach explicitly considers the increase in the effective conjugation length Δn of the polyynes when adding the end caps, and we proposed the function, $\gamma = a + b(n + \Delta n)^c$, with constant b and c determined from the uncapped polyynes. This can be compared with the conventional choice of $\gamma = a + bn^c$ (with freely varying a, b, and c values) which has been used in previous experimental and theoretical work. After fitting the new functional form to our theoretical data, we obtained Δn values for one TIPS and one phenyl end cap of ~0.83 and 1.35, respectively. For the phenyl end caps, our new power law gives a better fit to the theoretical data, as measured by the χ^2 value of the residual errors.

We also compared our results with the experimental c values of Ph–(C≡C)$_n$–Ph and i-(Pr)$_3$ Si–(C≡C)$_n$–Si i-(Pr)$_3$, obtained from the power-law $\gamma = a + bn^c$. Our HF and LC-DFT results underestimated the resulting c values, but this is consistent with previous theoretical studies. To attempt to explain the discrepancy, we estimated the vibrational contribution to the γ values within the double harmonic approximation, but found that the correction had no systematic effect on the c values, and in any case was rather small. Nevertheless, compared to previous theoretical studies, our improved c values were found to be somewhat larger and closer to experiment, and for the first time we have shown that theory can correctly predict that the c values of Ph–(C≡C)$_n$–Ph are higher than those of i-(Pr)$_3$ Si–(C≡C)$_n$–Si i-(Pr)$_3$.

Finally, using the experimental γ values, we estimated the c value of uncapped polyynes, which has not been determined experimentally, on the assumption that two phenyl end caps increase conjugation length of polyynes by 2.7 (based on our new fitting model). We predict that the experimental c value will be ~4.88.

References

1. Zyss, J. Molecular Nonlinear Optics: Matericals, Physics, and Devices; Academic: New York, 1994; Chapter 6 and 10.
2. Nalwa, H. S.; Miyata, S. Molecular Nonlinear Optics of Organic Molecules and Polymers; CRC: Boca Raton, 1997; Chapter 11 and 12.
3. Zyss, J.; Chemla, D. S. Nonlinear Optical Properties of Organic Molecules and Crystals; Academic: Orlando, 1987; Chapter II-1, Chapter II-2, and Chapter III-5.
4. Kuzyk, M. G. SPIE Proc 1997, 3147, 128.
5. Kanis, D. R.; Ratner, M. A.; Karks, T. J. Chem Rev 1994, 94, 195.
6. Breitung, E. M.; Shu, C-F.; McMahon, R. J. J Am Chem Soc 2000, 122, 1154.
7. Kohn, W.; Sham, L. J. Phys Rev 1965, 140, A1133.
8. Parr, R. G.; Yang, W. Density-Functional Theory of Atoms and Molecules; Oxford University Press: New York, 1989.
9. Dreizler, R. M.; Gross, E. K. U. Density-Functional Theory: An Approach to the Quantum Many-Body Problem; Springer: Berlin, 1990.
10. Champagne, B.; Perpète, É. A.; Jaquemin, D.; van Gisbergen, S. J. A.; Baerends, E-J.; Soubra-Ghaoui, C.; Robins, K. A.; Kirtman, B. J Phys Chem A 2000, 104, 4755.
11. Champagne, B.; Perpète, É. A.; van Gisbergen, S. J. A.; Baerends, E-J.; Snijders, J. G.; Soubra-Ghaoui, C.; Robins, K. A.; Kirtman, B. J Chem Phys 1998, 109, 10489.

12. Sekino, H.; Maeda, Y.; Kamiya, M.; Hirao, K. J Chem Phys 2007, 126, 014107.
13. Song, J-W.; Watson, M. A.; Sekino, H.; Hirao, K. J Chem Phys 2008, 129, 024117.
14. Iikura, H.; Tsuneda, T.; Yanai, T.; Hirao, K. J Chem Phys 2001, 115, 3540.
15. Tawada, Y.; Tsuneda, T.; Yanagisawa, S.; Yanai, T.; Hirao, K. J Chem Phys 2004, 120, 8425.
16. Song, J-W.; Hirosawa, T.; Tsuneda, T.; Hirao, K. J Chem Phys 2007, 126, 154105.
17. Sato, T.; Tsuneda, T.; Hirao, K. J Chem Phys 2007, 126, 234114.
18. Song, J-W.; Tokura, S.; Sato, T.; Watson, M. A.; Hirao, K. J Chem Phys 2007, 127, 154109.
19. Song, J-W.; Watson, M. A.; Nakata, A.; Hirao, K. J Chem Phys 2008, 129, 184113.
20. Slepkov, A. D.; Hegmann, F. A.; Eisler, S.; Elliott, E.; Tykwinski, R. R. J Chem Phys 2004, 120, 6807.
21. Eisler, S.; Slepkov, A. D.; Elliott, E.; Luu, T.; McDonald, R.; Hegmann, F. A.; Tykwinski, R. R. J Am Chem Soc 2005, 127, 2666.
22. Luu, T.; Elliott, E.; Slepkov, A. D.; Eisler, S.; McDonald, R.; Hegmann, F. A.; Tykwinski, R. R. Org Lett 2005, 7, 51.
23. Becke, A. D. Phys Rev A 1988, 38, 3098.
24. Tsuneda, T.; Suzumura, T.; Hirao, K. J Chem Phys 1999, 110, 10664.
25. NIST Computational Chemistry Comparison and Benchmark Database, Release 14, Sep 2006, NIST Standard Reference Database 101. Available at http://srdata.nist.gov/cccbdb/.
26. Jaquemin, D.; Champagne, B.; André, J-M. Int J Quantum Chem 1997, 65, 679.
27. Dunning, T. H., Jr. J Chem Phys 1989, 90, 1007.
28. Frisch, M. J.; Trucks, G. W.; Schlegel, H. B.; Scuseria, G. E.; Robb, M. A.; Cheeseman, J. R.; Montgomery, J. A., Jr.; Vreven, T.; Kudin, K. N.; Burant, J. C.; Millam, J. M.; Iyengar, S. S.; Tomasi, J.; Barone, V.; Mennucci, B.; Cossi, M.; Scalmani, G.; Rega, N.; Petersson, G. A.; Nakatsuji, H.; Hada, M.; Ehara, M.; Toyota, K.; Fukuda, R.; Hasegawa, J.; Ishida, M.; Nakajima, T.; Honda, Y.; Kitao, O.; Nakai, H.; Klene, M.; Li, X.; Knox, J. E.; Hratchian, H. P.; Cross, J. B.; Bakken, V.; Adamo, C.; Jaramillo, J.; Gomperts, R.; Stratmann, R. E.; Yazyev, O.; Austin, A. J.; Cammi, R.; Pomelli, C.; Ochterski, J. W.; Ayala, P. Y.; Morokuma, K.; Voth, G. A.; Salvador, P.; Dannenberg, J. J.; Zakrzewski, V. G.; Dapprich, S.; Daniels, A. D.; Strain, M. C.; Farkas, O.; Malick, D. K.; Rabuck, A. D.; Raghavachari, K.; Foresman, J. B.; Ortiz, J. V.; Cui, Q.; Baboul, A. G.; Clifford, S.; Cioslowski, J.; Stefanov, B. B.; Liu, G.; Liashenko, A.; Piskorz, P.; Komaromi, I.; Martin, R. L.; Fox, D. J.; Keith, T.; Al-Laham, M. A.; Peng, C. Y.; Nanayakkara, A.; Challacombe, M.; Gill, P. M. W.; Johnson, B.; Chen, W.; Wong, M. W.; Gonzalez, C.; Pople, J. A. Gaussian 03, Revision D. 02, Gaussian, Inc.: Wallingford, CT, 2004.
29. Agren, H.; Angeli, C.; Bak, K. L.; Bakken, V.; Christiansen, O.; Cimiraglia, R.; Coriani, S.; Dahle, P.; Dalskov, E. K.; Enevoldsen, T.; Fernandez, B.; Haettig, C.; Hald, K.; Halkier, A.; Heiberg, H.; Helgaker, T.; Hettema, H.; Jensen, H. J. A.; Jonsson, D.; Joergensen, P.; Kirpekar, S.; Klopper, W.; Kobayashi, R.; Koch, H.; Ligabue, A.; Lutnaes, O. B.; Mikkelsen, K. V.; Norman, P.; Olsen, J.; Packer, M. J.; Pedersen, T. B.; Rinkevicius, Z.; Rudberg, E.; Ruden, T. A.; Ruud, K.; Salek, P.; Sanchez de Meras, A.; Saue, T.; Sauer, S. P. A.; Schimmelpfennig, B.; Sylvester-Hvid, K. O.; Taylor, P. R.; Vahtras, O.; Wilson, D. J. Dalton. A Molecular Electronic Structure Program. Release 2.0, 2005. Available at http://www.kjemi.uio.no/software/dalton/dalton.html.
30. Slepkov, A. D.; Hegmann, F. A.; Zhao, Y.; Tykwinski, R. R.; Kamada, K. J Chem Phys 1993, 98, 7229.
31. Perpète, É. A.; Champagne, B.; André, J-M.; Kirtman, B. J Mol Struct 1998, 425, 115.
32. Kirtman, B.; Champagne, B. Int Rev Phys Chem 1997, 16, 389.
33. Jaszuński, M.; J&uhook;rgensen, P. H.; Koch, H. Ågren, Helgaker, T. J Chem Phys 1993, 98, 7229.
34. Kirtman, B. Int J Quantum Chem 1992, 43, 147.
35. Ray, P. C. Chem Phys Lett 2004, 395, 269.
36. Buma, W. J.; Fanti, M.; Zerbetto, F. Chem Phys Lett 1999, 313, 426.
37. Archibong, E. F.; Thakkar, A. J. J Chem Phys 1993, 98, 8324.